IUCAA - 7 /95
March 95

A Modified Periodogram for the Detection of Gravitational Waves from Coalescing Binaries

By

S.D. Mohanty and B.S. Sathyaprakash

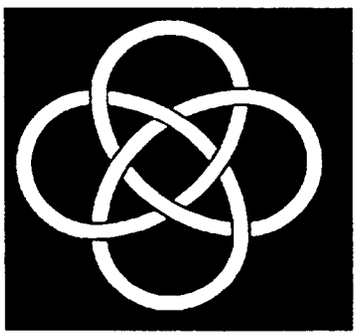

Inter-University Centre for Astronomy & Astrophysics

An Autonomous Institution of the University Grants Commission

Preprint Request (Please quote the preprint number)
email : preprn@iucaa.ernet.in
Fax : 0212 - 335760
Post : IUCAA, Post Bag 4, Ganeshkhind, Pune 411 007, India.

A modified periodogram for the detection of gravitational waves from coalescing binaries

S.D. Mohanty and B.S. Sathyaprakash
Inter-University Centre for Astronomy and Astrophysics, Post Bag 4, Ganeshkhind Pune 411 007, India

Weiner filtering a signal from a noisy detector output is a well known technique and is envisaged to be used in the detection and analysis of gravitational waves emitted during mergers of compact binaries consisting of neutron stars or black holes as their components. Even though a Weiner filter is the most optimal linear filter there is a necessity for the development of computationally less intensive and/or statistically independent strategies of detection. In this paper we have investigated the feasibility of a technique called periodogram analysis vis a vis Weiner filtering. We find that the two techniques yield the same signal-to-noise ratio, are computationally equally expensive and are statistically independent. These results imply that in the detection problem one can use either a periodogram or a Weiner filter and if a signal is detected by both these techniques, one can be more confident about its presence.

I. INTRODUCTION

In a few years from now several interferometric gravitational wave detectors, two large scale interferometers in the US [1], one large interferometer in Italy [2] and possibly a few more smaller ones elsewhere, are expected to become operational. A primary source for these detectors is the gravitational radiation burst emitted during the coalescence of a compact binary system [3]. Except for binaries located in our own Galaxy, the raw amplitude of these signals may not be large enough for the signal to be visible in the time-series above the detector noise. However, since the wave form from these sources can be modeled very accurately it is possible to enhance the signal-to-noise ratio by employing special data analysis techniques like optimal Weiner filtering [3,4]. In the time series one is comparing the signal power with that of noise while Weiner filtering essentially allows us to compare the energy of the signal with that of the noise. This is achieved by correlating the detector output with a filter which in the Fourier domain is a copy of the signal weighted by the noise power spectrum. The signal when present in the data train would correlate very well with such a filter while the noise on the average does not, so that the filter in effect efficiently picks up all the signal power without picking up the noise power as efficiently. As a result there can be a tremendous enhancement in the signal-to-noise ratio. For example, at a distance of about 100 Mpc, the first generation of VIRGO and LIGO detectors might observe coalescing binary events with a signal-to-noise ratio (SNR) $\sim$ 10 (see e.g. [5]) with the aid of matched filtering technique; and future "advanced detectors" could achieve very large SNRs indeed [6]. In practice we would not know when the signal arrives or what its parameters are so that it is necessary to correlate each piece of data with a host of templates each corresponding to a different set of signal parameters and which together span the relevant range of parameters. When we use a discrete lattice of templates it is obvious that in general none of them will perfectly match an incoming signal and hence there will be a substantial drop in the signal-to-noise ratio. Moreover, it is crucial to know the time evolution of the phase of the signal accurately as otherwise the template and the signal will go out of phase even when the parameters are matched [7–9]. Thus, the wave form needs to be computed by incorporating higher order general relativistic corrections. When these corrections are taken into account the parameter space of the signal acquires an extra dimension. This leads to a substantial increase in the number of templates, though by a judicious choice of signal parameters it may still be possible, for the purpose of detection, to work with the same number of parameters as in the lowest order approximation of the wave form [10]. There have been efforts in the past in devising 'trigger' algorithms that are computationally less intensive but such algorithms work at the cost of the SNR and thus with a substantial enhancement in the false alarm probability [11].

Signal analysis is thus a major component in the detection of gravitational radiation and in the subsequent extraction of useful astrophysical information. It is therefore necessary to develop algorithms that are all as powerful as matched filtering but complementary to one another in the sense of being statistically independent so that the confidence level of detection improves substantially. In this paper we propose an algorithm called a *periodogram* to detect gravitational radiation from coalescing binaries which is complementary to the work of Smith [12]. Periodograms are routinely used by radio astronomers in enhancing the signal-to-noise ratio of radio signals from pulsars [13]. The basic idea of a periodogram is very simple: Suppose we have a sinusoidal signal present in a very noisy data. If we know the exact period of the sinusoid then we can fold the data after every cycle and in the folded data the sinusoid would keep building up in proportion to the number of foldings while the noise, being uncorrelated, builds up much more slowly — in proportion to the square root of the number

of foldings. Consequently if the signal lasts for n-cycles we would in effect increase the energy of the signal relative to noise by $\sqrt{n}$. Even when we do not know the exact frequency of the signal but are aware that its frequency lies in a certain range, we could successively try foldings at different time intervals corresponding to different interesting frequencies. We would eventually pick up the signal, whenever it is present, provided we have a sufficiently large number of cycles. We can use the same technique in the case of gravitational radiation from coalescing binaries but since the signal is not monochromatic we need to apply a modified version of the algorithm.

The rest of the paper is organized as follows. In Sec. II we briefly review the nature of the gravitational radiation emitted by coalescing binaries and introduce the notations and conventions followed in the rest of the paper. In Sec. III we present the periodogram analysis for coalescing binary signals and discuss various aspects of such an analysis: The periodogram algorithm is presented in Sec. III A. In Sec. III B we define the detection strategy, compute the detection and false alarm probabilities and derive an expression for the signal-to-noise ratio obtained using this strategy. In order to estimate the computational costs of the periodogram in picking up arbitrary signals one needs to understand how the signal-to-noise ratio falls as the parameters used in constructing the periodogram are mismatched with those of a signal. This will be presented in the latter half of Sec. III B. Numerical implementation of the periodogram is presented in Sec. III C. We conclude Sec. III by estimating the computational costs involved in using a periodogram. In Sec. IV we compare the periodogram with Weiner filtering and show that the two techniques (i) yield the same signal-to-noise ratio, (ii) are computationally equally expensive and (iii) are statistically independent. The first two of these points imply that in the detection problem we can use either a periodogram or a Weiner filter and the last one implies that if a signal is detected by both these techniques then we can be more confident about its presence. In Sec. V we summarize the main results of our work.

II. CHIRP WAVE FORM

In this Section we briefly discuss the nature of the gravitational wave emitted by a binary system of stars, often called a chirp wave form, and collect formulas relevant to the discussion of periodogram and matched filtering. No effort is made to cover the exhaustive literature that is now available on the accurate modeling of the in-spiral radiation from binary systems, taking into account higher order post-Newtonian corrections (see, for instance, Blanchet et al. [14]).

In the quadrupole approximation, gravitational waves from a binary system of stars modeled as point masses orbiting about each other in a circular orbit, induce a strain $h(t)$ at the detector given by (see e.g. [3]) [15]

$$h(t) = \mathcal{N} q(t) = \mathcal{N}(\pi f(t))^{2/3} \cos[\varphi(t) + \Phi] \qquad (1)$$

where $\mathcal{N}$ is a constant for a given binary involving distance to the binary, its reduced and total mass, and the antenna pattern of the detector. The detailed form of $\mathcal{N}$ will not be of any concern in this paper; we choose $\mathcal{N}$ so as to normalize the energy of the signal in the frequency band of interest (see eqn (6) below). The instantaneous gravitational wave frequency, equal to twice the orbital frequency of the binary, is given by

$$f(t) = f_a \left[1 - \frac{t - t_a}{t_C}\right]^{-3/8}, \qquad (2)$$

where t_C is a constant having dimensions of time

$$t_C = \frac{5}{256} \mathcal{M}^{-5/3} (\pi f_a)^{-8/3}, \qquad (3)$$

and f_a and Φ are the frequency and the phase of the signal, respectively, at $t = t_a$. In the quadrupole approximation the time-dependent phase of the wave form is given by

$$\varphi(t) \equiv 2\pi \int_0^t f(t) dt = \frac{16\pi f_a t_C}{5} \left[1 - \left(\frac{f(t)}{f_a}\right)^{-5/3}\right]. \qquad (4)$$

We shall refer to the time elapsed starting from an epoch when the gravitational wave frequency is f_a till the epoch when it becomes infinite, at which time the two stars would theoretically coalesce, as the *chirp time* of the signal. From equation (2) we see that t_C is the chirp time. The phase of the signal (4) is essentially characterized by three parameters: (i) the *time-of-arrival* t_a when the signal first becomes *visible* in the detector, (ii) the *phase* Φ of the signal at the time-of-arrival and (iii) the *chirp mass* $\mathcal{M} = (\mu^3 M^2)^{1/5}$, where μ and M are the reduced and the total mass of the binary, respectively. Note that at this level of approximation the phase (as also the amplitude) depends on the masses of the two stars only through the above combination of the individual masses. Consequently, two coalescing binary signals of the same chirp mass but of different sets of individual masses would be degenerate and thus exhibit exactly the same time evolution.

We end this Section by defining the scalar product of wave forms. Given two wave forms $g(t)$ and $h(t)$ their scalar product is defined by

$$\langle g, h \rangle \equiv \int_{-\infty}^{\infty} \frac{\tilde{g}(f)\tilde{h}^*(f)}{S_n(f)} df \qquad (5)$$

where $S_n(f)$ is the *two-sided* detector noise power spectral density and $\tilde{g}(f) = \int_{-\infty}^{\infty} g(t) \exp(2\pi i f t) dt$ and $\tilde{h}(f) = \int_{-\infty}^{\infty} h(t) \exp(2\pi i f t) dt$, are the Fourier transforms

of the wave forms $g(t)$ and $h(t)$, respectively. A wave form is said to be *normalized* if its norm computed using the above definition of the scalar product is unity. We refer to normalized wave forms as signals of *unit strength*. The normalisation constant for signals of unit strength is given by

$$\langle h, h\rangle = 1 \Longrightarrow \mathcal{N} = \langle q, q\rangle^{-1/2}. \tag{6}$$

Consistent with the above definition, a signal $s(t)$ of strength s_0 is given by

$$s(t) = s_0 h(t);\ \langle s, s\rangle^{1/2} = s_0, \tag{7}$$

where $h(t)$ is a normalized wave form. We will now see how the periodogram works.

III. PERIODOGRAM

In the Introduction we briefly mentioned the idea of a periodogram and indicated how it may be applied to sinusoidal signals buried in noisy data. Radio signals from a pulsar are periodic in the rest frame of the pulsar but an observer at Earth receives a Doppler modulated signal due to the relative motion of the pulsar and the Earth. Consequently, one cannot fold a pulsar signal at regular intervals. However, since we know the motion of the Earth to a good degree of accuracy it is possible to correct for Doppler modulation by an appropriate resampling of the data so that the resampled data would contain pulses at regular intervals. In this case one complication for data analysis is that the Doppler modulation depends on the location of the pulsar, being the least for pulsars located along the Earth's spin axis (and not zero, since Earth's motion about Sun and Moon might still contribute significantly). Thus, while searching for unknown pulsars one has to try several Doppler de-modulations.

For gravitational waves from coalescing binaries, Doppler modulation of the signal due to Earth's motion could be very crucial, especially at low values ($\sim$ 10−40 Hz) of the seismic cutoff since the integration time in that case could be $\sim$ few hours. However, for large values of the seismic cutoff the time scale over which a signal lasts, being at most a few minutes, would be too small compared to typical time scales in the Earth's motion. Even if this effect were neglected, chirp signals cannot be folded at regular intervals because of their intrinsic non-periodicity. What one can do in this case is to initially sample the data at a very high rate and at regular intervals and to then resample at a rate at which the phase of the signal is increasing. An appropriate resampling would render the signal to be periodic which can then be folded to enhance the signal-to-noise ratio.

In this Section we discuss how a periodogram can be applied to non-monochromatic signals. In the first part of this Section we present the algorithm, followed by a discussion of the power of the test, optimal SNR achievable using this strategy and the *ambiguity function* which is a measure of the robustness of the algorithm. In the last two parts we discuss numerical implementation and computational costs concerning this technique.

A. Algorithm

Let $h(t;\lambda)$ denote a chirp wave form of unit strength parametrized by $\lambda = (\lambda_1, \lambda_2, \ldots, \lambda_n)$. For the quadrupole wave form given by equation (1) the parameters are given by either the set $\lambda = (t_a, \Phi, \mathcal{M})$ or the set $\lambda = (t_a, \Phi, t_C)$. We shall find the latter set to be more appropriate in our discussions below. If instead of t a new time variable τ defined by

$$\tau \equiv \frac{\varphi(t;\lambda)}{2\pi f_0}, \tag{8}$$

where f_0 is an arbitrary constant having dimension of frequency, is used then the wave form (1) appears as an amplitude modulated, truncated cosine wave:

$$h(t) \longrightarrow h(\tau) = \mathcal{N} f^{2/3}(\tau)\cos(2\pi f_0 \tau + \Phi);\ 0 \le \tau \le \tau_C \tag{9}$$

where τ_C is the chirp time in the new time coordinate

$$\tau_C = \frac{8 f_a t_C}{5 f_0}. \tag{10}$$

Such a transformation of the time variable which renders the chirp wave form as a sinusoidal signal was first considered by Smith [12] (see also the discussion in Schutz [4]). Our analysis differs from that of Smith from here onwards: Smith suggests Fourier analysis of the transformed data while we construct a *periodogram* by folding data after each cycle and adding the resultant cycles. If for the moment we ignore that the amplitude of the chirp signal is increasing with time then the enhancement in the amplitude of the signal after repeated folding and adding is just the number of cycles $N_{\rm cyc}$ of the signal in the interval t_C. For chirp signals, $N_{\rm cyc}$ can easily be read off from equation (4):

$$N_{\rm cyc} \equiv \frac{\varphi(t_C + t_a) - \varphi(t_a)}{2\pi} = f_0 \tau_C. \tag{11}$$

The data from a detector will also contain noise so that the signal-to-noise ratio will only increase, as we shall see below, in proportion to $\sqrt{N_{\rm cyc}}$. After obtaining the periodogram we can correlate it with a sinusoid of frequency f_0. The result of such an operation is the statistic on which we set a threshold to decide whether or not a signal is present in the detector output. It is to be expected that even when there is a slight mismatch in the

parameters used in the time transformation equation (8) and those of the signal, the resulting periodogram will be close to a sinusoidal wave form. In Fig. 1 we have shown how the phase of a mismatched wave form develops relative to that of a perfectly matched one, as a function of τ. We see that even when there is as much as a 20 ms difference in chirp times, the two wave forms have only gone out of phase by one cycle. This is reassuring since one does not have to use too many test values of chirp times in constructing a periodogram when we do not know the parameter values of the signal. We shall formulate this problem more precisely in Sec. III B. We now consider how the detector noise behaves when a periodogram is constructed and express much of the above formally.

Let $x(t)$ denote the detector output. Given $x(t)$, we have two possibilities: $x(t)$ is just an instance of noise or it contains a signal $s(t;\hat{\lambda})$ of strength s_0 :

$$x(t) = \begin{cases} n(t), & \text{in the absence of any signal,} \\ n(t) + s(t;\hat{\lambda}), & \text{when a signal is present.} \end{cases} \tag{12}$$

We assume that the noise is a Gaussian random process of mean zero and covariance

$$\overline{n(t)n(t')} = \sigma^2\delta(t-t') \tag{13}$$

where an overbar denotes the ensemble average.

In the detection problem, $x(t)$ is given and a decision has to be made about the presence or absence of a signal, irrespective of its parameters. If it is known that only one kind of signal having parameters $\hat{\lambda}$ occurs, then one could transform to a new time $\tau = \varphi(t;\hat{\lambda})/2\pi f_0$ and fold the data over every increment $1/f_0$ in $\tau(t;\hat{\lambda})$ starting from $\tau = 0$ till some $\tau \leq \tau_C$. From equations (9), (11) and (13) it follows that, if such a signal is present, the result will be a sinusoidal wave form of period $1/f_0$ embedded in white noise of variance $\sqrt{N_{\rm cyc}}\sigma$ (cf. (16)). But, in practice, the parameters of the signal are a priori unknown and it is necessary to transform the data to a new time coordinate τ using a number of test parameters ${}_t\lambda_k$, $k = 1,\ldots n$, which together span the range of signal parameters. For each ${}_t\lambda$, the operations of *time transformation, folding* and *adding* yield a periodogram, $X(\tau;{}_t\lambda)$ [16]:

$$X(\tau;{}_t\lambda) = \sum_{j=0}^{N_{\rm cyc}-1} x\left(t(\tau;{}_t\lambda)\right)\Pi(\tau f_0 - j), \quad 0 \leq \tau < 1/f_0, \tag{14}$$

where Π is defined by

$$\Pi(\tau f_0 - j) = \begin{cases} 1, & \text{if } j \leq \tau f_0 < (j+1) \\ 0, & \text{otherwise.} \end{cases} \tag{15}$$

In general the periodogram of the noisy detector output, constructed using a set of test parameters ${}_t\lambda$, will be:
(a) white noise, if no signal is present

$$X(\tau;{}_t\lambda) = N(\tau), \quad \overline{N(\tau)N(\tau')} = N_{\rm cyc}\sigma^2\delta(\tau-\tau'); \tag{16}$$

(b) an amplitude modulated sinusoid with an unknown phase Φ embedded in white noise, if the test parameters ${}_t\lambda$ happen to match the parameters $\hat{\lambda}$ (up to a phase) of the signal actually present in $x(t)$

$$X(\tau;{}_t\lambda) = N(\tau) + S(\tau), \tag{17}$$

where the periodogram $S(\tau)$ is given by

$$S(\tau) = N_{\rm cyc}s_0\mathcal{N}\overline{A}(\tau)\cos(2\pi f_0\tau + \Phi); \tag{18}$$

with $\overline{A}(\tau)$ the amplitude of the periodogram when its phase is $2\pi f_0\tau$ computed by averaging the signal amplitude over all the cycles:

$$\overline{A}(\tau) = \frac{1}{N_{\rm cyc}}\sum_{j=0}^{N_{\rm cyc}-1}\left[\pi f\left(t(\tau + jf_0^{-1})\right)\right]^{2/3}; \tag{19}$$

and
(c) a non-sinusoidal wave form embedded in white noise, if there is a mismatch in the two sets of parameters.

As we have argued earlier, for a small mismatch in the parameters, the periodogram is still a sinusoid, possibly with a reduced amplitude and a phase different from the true phase of the signal. In Fig. 2 we have shown the development of the periodogram amplitude $\overline{A}(\tau)$, normalized to $\overline{A}(0)$, for the case of a perfect matching of parameters and for several values of the chirp time. In computing $\overline{A}(\tau)$ we have taken 95% of the total number of cycles. It turns out that the amplitude $\overline{A}$ of the periodogram is roughly a constant though the signal amplitude is a function of time, rapidly increasing at times close to coalescence. The amplitude increase is larger, lower the chirp time. Even in the case of $t_C = 1$ s the increase is only about 1%.

This result follows from the fact that the signal amplitude does not change appreciably over one cycle and the periodogram amplitude is obtained by averaging the former over many cycles.

B. Detection probability and ambiguity function

The transformation from $t \longrightarrow \tau$ depends on the parameters of the signal we wish to detect. A mismatch in the parameters of the signal and those used in the transformation causes the SNR to fall below the optimal value obtainable when the two sets of parameters are perfectly matched. As discussed earlier we would not know apriori what the chirp time of the signal is nor would we know when it arrives. Consequently, we need to compute the periodogram and the corresponding SNR for several test values of the chirp time and for each piece of data. The issues we address in this Section concern the number of test values of chirp times we need to use for a given data

train and size of step in the time-of-arrival we can afford without an appreciable loss in the SNR.

Let us first consider the simple case of a family of signals, all having the same parameters $\hat{t}_a$ and $\hat{t}_C$ but differing in Φ - the initial phase. Then the signal detection problem, after obtaining the periodogram, reduces to that of detecting a sinusoid of unknown phase in white noise. As has been mentioned before, the most optimum strategy in such a case is to perform matched filtering [17]. But the phase of the sinusoid being unknown, a search in Φ will have to be performed. This, however, does not imply that periodograms for all Φ between 0 and 2π are required, for the following reason. The periodogram will yield a sinusoid of unknown phase

$$\begin{aligned} S(\tau;\Phi) &= S_0 \cos(2\pi f_0 \tau + \Phi) \\ &= S_0 \left[\cos\Phi \cos(2\pi f_0 \tau) - \sin\Phi \sin(2\pi f_0 \tau)\right] \end{aligned} \tag{20}$$

where $S_0 = N_{\mathrm{cyc}} s_0 \mathcal{N} \overline{A}$. Thus, the signal to be detected is just a linear combination of two orthogonal vectors $\cos(2\pi f_0 \tau)$ and $\sin(2\pi f_0 \tau)$. Hence, only the projections of the periodogram onto these two are required and a sum of their squares will yield the desired correlation. Therefore, the detection statistic required is

$$G(\hat{\lambda}) = \sqrt{C_0^2 + C_{\frac{\pi}{2}}^2} \tag{21}$$

which must be compared with a threshold G_0, where

$$C_0(X;\hat{\lambda}) = \int_0^{1/f_0} X(\tau) \cos(2\pi f_0 \tau(t;\hat{\lambda}))d\tau, \tag{22}$$

$$C_{\frac{\pi}{2}}(X;\hat{\lambda}) = \int_0^{1/f_0} X(\tau) \sin(2\pi f_0 \tau(t;\hat{\lambda}))d\tau. \tag{23}$$

The statistic $G(\hat{\lambda})$ is not a Gaussian random variable anymore. Its probability distribution functions $p_0(G)$ and $p_1(G)$, in the absence and the presence of the signal are the well known Rayleigh and Rician distributions, respectively, [18]:

$$p_0(G) = \frac{G}{\sigma_p^2} \exp\left(-\frac{G^2}{2\sigma_p^2}\right) \quad G \geq 0 \tag{24}$$

$$p_1(G) = \frac{G}{\sigma_p^2} \exp\left(-\frac{(G^2/\sigma_p^2) + \rho^2}{2}\right) I_0(G\rho/\sigma_p) \tag{25}$$

where σ_p^2 is the variance of the statistics C_0 and $C_{\frac{\pi}{2}}$ given by

$$\sigma_p^2 = N_{\mathrm{cyc}} \sigma^2 \int_0^{1/f_0} \cos^2(2\pi f_0 \tau(t;\lambda))d\tau, \tag{26}$$

$I_0(z)$ is the modified Bessel function of the first kind of order zero and,

$$\rho = \frac{S_0}{\sqrt{N_{\mathrm{cyc}}}\sigma} \sqrt{\int_0^{1/f_0} \cos^2(2\pi f_0 \tau)d\tau}. \tag{27}$$

The false alarm and the detection probabilities, which are just the integrals of $p_0(G)$ and $p_1(G)$ from $G = G_0$ to ∞, are given by

$$Q_0(G_0) = \exp\left(-\frac{G_0^2}{2\sigma_p^2}\right) \tag{28}$$

$$Q_d(G_0) = \int_{G_0/\sigma_p}^{\infty} \exp\left(-\frac{x^2+\rho^2}{2}\right) I_0(x\rho) x \, dx. \tag{29}$$

Thus ρ is the SNR for this strategy. For $\rho = 0$, the detection and false alarm probabilities become equal. Altough ρ is equal in magnitude to the SNR of the optimal strategy for detecting a signal of *known* phase, the functional forms of Q_0 and Q_d are different for the latter. Only for high ρ (≥ 6) are the *operating characteristics* nearly identical for the two cases (for details, see [18]).

An a priori knowledge of the distribution of the parameters, assumed in the above, will not be available of course. The most optimum strategy then is to construct periodograms for a set of test values ${}_t\lambda$ of the parameters, compute the corresponding $G({}_t\lambda)$ and find the values of parameters ${}_m\lambda$ which maximize G. If the maximum crosses a preset threshold then a detection is announced. The corresponding parameters are measured values of the signal parameters. At this point a word of caution is in order: The *best estimate* of the actual signal parameters need not be ${}_m\lambda$ because of correlations which exist among the errors in t_a, t_C and Φ. Thus, even though a mismatch in t_a alone will reduce G, a mismatch in t_C along with t_a may cause a lesser reduction. In fact, such correlations help us as far as just detection is concerned by reducing the number of points in the parameter space that need be sampled in a search. In order to determine whether the values measured in this way give an unbiased and minimal uncertainty estimate it would be necessary to compute the distribution of the measured values. We relegate this important problem to a future work.

Sampling is unavoidable as it is impossible, in practice, to perform a search over the *continuum* of the t_a-t_C space. This means that there will always, in general, be a mismatch between the parameters used in constructing a periodogram and those of the actual signal which may be present. Hence, we must consider now a detection strategy which uses not the true parameters but a slightly mismatched set. The signal-to-noise ratio for such a detection strategy can be computed in a manner analogous to that of the case treated above and it turns out to be

$$\rho(\hat{\lambda},\lambda) = \frac{\left(\overline{C}_0^2 + \overline{C}_{\frac{\pi}{2}}^2\right)^{1/2}}{\sigma_p} \tag{30}$$

where $\hat{\lambda}$ are the true parameters, λ are the ones used to construct the periodogram and

$$\overline{C}_0(\hat{\lambda}, {}_t\lambda) = \int_0^{1/f_0} S(\tau; \hat{\lambda}, {}_t\lambda) \cos(2\pi f_0 \tau) d\tau; \qquad (31)$$

$$\overline{C}_{\frac{\pi}{2}}(\hat{\lambda}, {}_t\lambda) = \int_0^{1/f_0} S(\tau; \hat{\lambda}, {}_t\lambda) \sin(2\pi f_0 \tau) d\tau. \qquad (32)$$

Here $S(\tau; \hat{\lambda}, {}_t\lambda)$ is the periodogram of the signal $s(t; \hat{\lambda})$ constructed using a set of test parameters ${}_t\lambda$ not necessarily matched on to the signal parameters $\hat{\lambda}$ and hence it need not be a sinusoid. The spacing between the sample points can now be fixed if a requirement is placed that every signal must have a detection probability $Q_d \geq$ some $Q_{d,min}$. The lower bound on Q_d places a lower bound on $\rho(\hat{\lambda}, \lambda)$ say κ. Thus, the sample points must be chosen in such a way that every point on the t_a—t_C plane falls within a ρ neighborhood, of radius κ, of at least one sample point. Fig. 3 shows the contours of equal $\rho(\hat{\lambda}, \lambda)$ computed for values of the periodogram parameters $t_a = 0$ s and $t_C = 0.8$ s, using a range of values of the signal parameters $-0.01 \text{ s} \leq \hat{t}_a \leq 0.01$ s and $0.79 \text{ s} \leq \hat{t}_C \leq 0.81$ s. In obtaining this figure we have chosen an upper frequency cutoff $f_c = 500$ Hz. At this cutoff more than 93% of the cycles are extracted. We have normalized ρ to unity at $\hat{t}_a = t_a$ and $\hat{t}_C = t_C$. The innermost contour corresponds to $\rho(\hat{\lambda}, \lambda) = 0.95$ and the value of $\rho(\hat{\lambda}, \lambda)$ reduces by 0.05 for successive outer contours. The innermost contours are closely approximated by ellipses. Area of an ellipse at a level $\kappa < 1$ gives *area* in the parameter space which the periodogram under consideration spans by obtaining on the average an SNR greater than κ times the optimal SNR. These ellipses are contours of what is known as the *ambiguity function* in the theory of microwave communication.

Since the ellipses are quite eccentric a particular periodogram spans a relatively large range of one of the parameters (either t_a or t_C) while a finer spacing will be necessary in the other direction. To be more specific, if the semi-major axis of an ellipse gives the span of a periodogram, say, in the direction of the chirp time, then the semi-minor axis gives its span in the direction of the time-of-arrival. For instance, by choosing $\kappa = 0.95$ we can afford a spacing of 10 ms in the time-of-arrival while the spacing in the chirp time can be no more than about a ms. Finally, we would like to remark that we obtain roughly the same behavior of $\rho(\hat{\lambda}, \lambda)$ irrespective of what value we use for λ. This means that the area in the parameter space spanned by any periodogram will be independent of the test values of the parameters that are used in constructing it.

C. Numerical Implementation

In data analysis problems we do not deal with a continuous signal but only a set of its discrete samples. Let δ denote the sampling interval (i.e. the constant interval between two consecutive samples) and $\{x_k\}$ the n samples of the detector output $x(t)$:

$$x_k \equiv x(t_k); \quad t_k \equiv k\delta; \quad k = 0, \ldots, n-1. \qquad (33)$$

In the presence of a signal whose samples are s_k we have

$$x_k = n_k + s_k \qquad (34)$$

where n_k are the samples of noise. Transforming to a new time variable τ and sampling the detector output uniformly in the transformed time variable means that we *resample* the data train at non-uniform intervals in terms of t. In what follows we denote the samples of the detector output (and other quantities) taken at uniform intervals Δ in the new time coordinate τ using an upper case Latin index. With this notation the detector output sampled uniformly in τ and in t are denoted by $\{x_K\}$, $K = 0, \ldots, N-1$ and $\{x_k\}$, $k = 0, \ldots, n-1$, respectively. We first estimate the sampling rate $f_s = \delta^{-1}$ needed in order to construct the samples $\{x_K\}$ from the samples $\{x_k\}$. Whenever a signal is present in the detector output, let us suppose we intend to have p points per cycle ($p \geq 2$) in τ. If we choose the detector upper frequency cutoff to be f_c then we must at least have $f_s = pf_c$. This means that at lower frequencies $f < f_c$ we will have more than p points per cycle in t. Consequently, the set $\{x_K\}$ will contain fewer points than the set $\{x_k\}$; i.e. $N \ll n$. For $f_c = 1$ kHz and $p = 8$, $f_s = 8$ kHz. Using the time transformation eqn (8) it is straightforward to deduce that the samples $\{x_K\}$ are related to $\{x_k\}$ by

$$x_K = x_j; \; j = \mathrm{I}\left[\frac{t_K}{\delta}\right], \qquad (35)$$

where I[ ] denotes the nearest integer of the quantity enclosed and t_K is given by

$$t_K = t_a + t_C \left[1 - \left(1 - \frac{K\Delta}{\tau_C}\right)^{8/5}\right]. \qquad (36)$$

It is to be noted that the equality between x_K and x_j is only an operational one and will be exact only in the limit when we have infinitely many samples in t. Having constructed the samples $\{x_K\}$ from the samples $\{x_k\}$ we next consider the periodogram of the set $\{x_K\}$ by folding it after every p samples and adding all the resultant N_{cyc} cycles. The resulting quantity is the (discrete) periodogram denoted by X_A,

$$X_A = \sum_{K=0}^{N_{\text{cyc}}-1} x_{pK+A}; \quad A = 0, \ldots, p-1. \qquad (37)$$

If we express the detector output in terms of noise plus the signal we get the analog of eqn (34)

$$X_A = N_A + S_A, \qquad (38)$$

where the N_A and S_A are periodograms of the noise and the signal, respectively, given by

$$N_A = \sum_{K=0}^{N_{cyc}-1} n_{pK+A}; \quad S_A = \sum_{K=0}^{N_{cyc}-1} s_{pK+A}. \tag{39}$$

It is straightforward to see that for noise n_i with covariance matrix $\overline{n_i n_j} = \sigma^2 \delta_{ij}$ the corresponding matrix of the periodogram of noise is given by

$$\overline{N_A N_B} = N_{\rm cyc} \sigma^2 \delta_{AB}. \tag{40}$$

Suppose a chirp wave form with chirp time $\hat{t}_C$ arrives at the detector at time $\hat{t}_a$. When the test parameters t_a and t_C (equivalently, τ_C) in eqn (36) perfectly match the parameters of the signal then the periodogram will be a single sinusoidal cycle of arbitrary phase:

$$S_A = N_{\rm cyc} s_0 \mathcal{N} \overline{A} \cos(2\pi A/p + \Phi) \tag{41}$$

where $\overline{A}$ is given by the discrete analog of expression (19). The normalization condition (6) in the case of white noise now translates to

$$\mathcal{N} = \frac{\sigma}{\overline{A}} \sqrt{\frac{2}{p N_{\rm cyc}}}. \tag{42}$$

where we have made use of the fact that the periodogram amplitude is roughly a constant. The statistic used for detecting such a signal, as discussed in the last section, is constructed out of the correlations C_0 and $C_{\frac{\pi}{2}}$ of the periodogram X_A with two sinusoids differing in phase by $\pi/2$

$$C_0 = \sum_{A=0}^{p-1} X_A \cos(2\pi A/p); \tag{43}$$

$$C_{\frac{\pi}{2}} = \sum_{A=0}^{p-1} X_A \cos(2\pi A/p + \pi/2). \tag{44}$$

Using the random variables C_0 and $C_{\frac{\pi}{2}}$ we can define the signal-to-noise ratio via

$$\rho \equiv \left(\mathcal{C}_0^2 + \mathcal{C}_{\frac{\pi}{2}}^2 \right)^{1/2} \tag{45}$$

where

$$\mathcal{C}_0^2 = \frac{\overline{C}_0^2}{\left(C_0 - \overline{C}_0\right)^2}; \quad \mathcal{C}_{\frac{\pi}{2}}^2 = \frac{\overline{C}_{\frac{\pi}{2}}^2}{\left(C_{\frac{\pi}{2}} - \overline{C}_{\frac{\pi}{2}}\right)^2}; \tag{46}$$

On substituting the expression for the periodogram of a chirp wave form of strength s_0 (cf. eqn (41)) we get

$$\overline{C}_0 = s_0 \sigma \sqrt{N_{\rm cyc} p/2} \cos\Phi; \quad \overline{C}_{\frac{\pi}{2}} = s_0 \sigma \sqrt{N_{\rm cyc} p/2} \sin\Phi; \tag{47}$$

and using (40) we obtain

$$\overline{\left(C_0 - \overline{C}_0\right)^2} = \overline{\left(C_{\frac{\pi}{2}} - \overline{C}_{\frac{\pi}{2}}\right)^2} = \sigma^2 N_{\rm cyc} p/2. \tag{48}$$

With the aid of the above expressions in (46) the SNR ρ is found to be

$$\rho = s_0. \tag{49}$$

Thus the signal-to-noise ratio obtained is simply equal to the strength s_0 of the signal itself. We shall later see that in the case of matched filtering too the SNR obtained is the same. In the next Section we compute the number of floating point operations involved in carrying out the periodogram analysis.

D. Computational costs of periodogram

In the previous sections we have seen how the SNR drops as the parameters used in constructing a periodogram are mismatched with those of a signal. The ambibuity function discussed in Sec. III B allows us to make a specific choice of test parameters for a given value of κ – the extent to which we allow the SNR to fall due to the discrete nature of the set of parameters used in the detection. For a chosen value of κ, the number of distinct periodograms $n_{\rm p}$ required in spanning a given region of the parameter space is roughly the total area of that region divided by the area of the ellipse A_κ corresponding to the value of κ. If the region of interest is a rectangle of sides $\Delta\lambda_i$ then

$$n_{\rm p} = \frac{\prod_i \Delta\lambda_i}{A_\kappa}. \tag{50}$$

For instance, if we take $\kappa = 0.9$ then the area enclosed by the corresponding ellispe (cf. Fig. 3) is $A_{0.9} \approx 2.6 \times 10^{-5} {\rm s}^2$. For $t_C \in [0, 4]$ s and $t_a \in [0, 12]$ s the number of periodograms required $\sim 2 \times 10^6$.

We now estimate the number of floating point operations per periodogram. If all the cycles are used in the analysis then the number of additions required are $p \times N_{\rm cyc}$, where p is the number of points per cycle in $\tau(t; {}_t\lambda)$. The number of multiplications required are much less at $2p$ and can be neglected in an order of magnitude calculation. For the range of the chirp time used above, the average number of additions required are

$$\frac{1}{4} \int_0^4 \frac{8 f_a t_C}{5} p dt_C \tag{51}$$

For $p = 8$ the number of additions required is 2560 . Therefore, the total number of floating point operations $N_{\rm PG}$ required in making a periodogram analysis of a data train 12 s long is

$$N_{\rm PG} = n_{\rm p} \times 2560 = 5 \times 10^9. \tag{52}$$

IV. COMPARISON OF MATCHED FILTERING AND PERIODOGRAM

In the foregoing Sections we have seen how to construct a periodogram, how many test values are needed in spanning the astrophysically relevant parameter space of chirp wave forms and what the computational costs involved are. In this Section we first discuss these aspects in the case of matched filtering and then indicate how the periodogram fares when compared to matched filtering.

The statistic used in the matched filtering technique is the correlation of the detector output with a family of templates corresponding to different values of the parameters. The SNR ρ obtained for a signal $s(t)$ using an optimal Weiner filter is simply the norm of the signal computed using the definition of the scalar product (5). Thus, the optimal SNR achieved for a signal $s(t)$, is its strength s_0 itself [19,6]:

$$\rho = \langle s, s \rangle^{1/2} = s_0. \tag{53}$$

Thus, the optimal SNR both in the case of periodogram and matched filtering are the same.

In the case of a Newtonian wave form it turns out that there is essentially only one parameter, viz the chirp time, for which Weiner filters are to be constructed explicitly; the time-of-arrival being taken care by the fast Fourier transform and the phase of the signal being extracted analytically using a two dimensional basis (see, for instance, ref. [4,19].) The templates required in chirp time can be determined by studying the behavior of the scalar product (cf. eqn (5)) of two chirp wave forms as a function of mismatch in their parameter values. Recall that the scalar product $C(\hat{\lambda}, {}_t\lambda)$ of two chirp wave forms $g(t; {}_t\lambda)$ and $h(t; \hat{\lambda})$ is given by

$$C(\hat{\lambda}, {}_t\lambda) = \left\langle g({}_t\lambda), h(\hat{\lambda}) \right\rangle. \tag{54}$$

Here $\hat{\lambda}$ can be thought of as the parameters of a signal while ${}_t\lambda$ those of a template. Then $C(\hat{\lambda}, {}_t\lambda)$ is the SNR obtained using a template whose chirp time is not necessarily the same as that of the signal. For simplicity we assume that the wave forms are of unit norm. Thus, $C(\hat{\lambda}, {}_t\lambda) = 1$, if $\hat{\lambda} = {}_t\lambda$ and $C(\hat{\lambda}, {}_t\lambda) < 1$, if $\hat{\lambda} \neq {}_t\lambda$. In the stationary phase approximation the Fourier transform of the Newtonian chirp wave form for positive frequencies is given by [3,19,6]

$$\tilde{h}(f) = \tilde{\mathcal{N}} f^{-7/6} \exp\left[i \sum_{k=1}^{3} \psi_k(f) \lambda_k - i \frac{\pi}{4} \right] \tag{55a}$$

where $\tilde{\mathcal{N}}$ is related to the normalisation constant $\mathcal{N}$ of the signal and

$$\psi_1(f) = 2\pi f, \tag{55b}$$

$$\psi_2(f) = 1, \tag{55c}$$

$$\psi_3(f) = 2\pi f - \frac{16\pi f_a}{5} + \frac{6\pi f_a}{5} \left(\frac{f}{f_a} \right)^{-5/3}. \tag{55d}$$

For $f < 0$ the Fourier transform is computed using the identity $\tilde{h}(-f) = \tilde{h}^*(f)$ obeyed by real functions $h(t)$. With the above expression for the Fourier transform the SNR (54), using (5), takes the form

$$C(\Delta\lambda) \propto \int_0^\infty \frac{f^{-7/3}}{S_n(f)} \cos\left[\sum_{k=1}^{3} \psi_k(f) \Delta\lambda_k \right] df \tag{56}$$

where $\Delta\lambda = \hat{\lambda} - {}_t\lambda$. In the stationary phase approximation the SNR is independent of the individual parameter values of the signal and the template: *For all signal-template pairs that have the same differences in times of arrival, phases, and chirp times one obtains the same SNR.* Consequently, constancy of the distance, measured using the scalar product (54), between two nearest neighbor filters translates into the constancy of the *distance*, measured using the difference in their parameter values.

$C(\Delta\lambda)$ traces out a three-dimensional surface as we vary $\Delta\lambda$. Since the time-of-arrival and the phase of the signal are not of relevance let us consider the curves $C(t_C, t_C^k)$ obtained by maximizing $C(\Delta\lambda)$, over t_a and Φ and varying the chirp time of the signal relative to the template. The curves so obtained are plotted for white noise (i.e. $S_n(f) = \text{const.}$) in Fig. 4, for templates of different chirp times by varying the chirp times of the signal. For the astrophysically relevant range of the masses of the two stars (say, $M_1, M_2 \in [0.5, 10]\ M_\odot$) and for $f_a = 100$ Hz, $t_C \in [12, 0.08]$ s. In Fig. 4 the chirp time is only varied over a portion of its relevant range.

How does one go about choosing the templates for the purpose of filtering the detector output? Let us start with the curve $C(t_C^1, t_C)$ corresponding to the left most template. (In what follows and in Fig. 4 $C(t_C^k, t_C)$ denotes the curve corresponding to the kth filter.) As the chirp time of the signal mismatches with that of the template the correlation function drops monotonically and at a 'distance' $\Delta_+ t_C^1$ from the first template it falls to a value, say, $\kappa < 1$. The chirp time t_C^2 of the second template is chosen in such a manner that for a signal of chirp time $t_C^1 + \Delta_+ t_C^1$, it too obtains an SNR equal to κ. With such a choice it is clear that all signals with their chirp times in the range $[t_C^1 - \Delta_- t_C^1, t_C^2 + \Delta_+ t_C^2]$ will be have an SNR $\geq \kappa$. In general, we require

$$C(t_C^k, t_C^k + \Delta_+ t_C^k) = C(t_C^{k+1}, t_C^{k+1} - \Delta_- t_C^{k+1}) = \kappa \tag{57}$$

where $\Delta_+ t_C^k$ ($\Delta_- t_C^k$) denotes the increment (decrement) in the chirp time of the kth template at which the correlation drops to a value κ. Since the correlation function only depends on the difference in chirp times and not on their absolute values (cf. equation (56)) we must have

$$\Delta_+ t_C^k = \Delta_- t_C^k = \Delta t_C^k; \quad \Delta t_C^k = \Delta t_C^j, = \Delta t_C \; \forall \; k, j. \quad (58)$$

Consequently, a constant spacing Δt_C between filters will do the job of uniformly covering the parameter space. As in the case of the periodogram if we allow for a drop $\kappa = 0.9$ in the SNR then the spacing between filters has to be $\Delta t_C = 5$ ms. In order to span the astrophysically interesting range of chirp times [0.08, 12] s we will need approximately 2×2400 templates where a factor of 2 arises since two filters for the parameter Φ are needed for every filter corresponding to t_C [19].

The computational cost of matched filtering has to be now ascertained. In the case of matched filtering we need only count the number of operations per filter and then multiply it by the total number of filters since, as opposed to periodogram, we do not explicitly have templates for the time-of-arrival. Given the samples o_k and q_k of a data train and a filter, respectively, the discrete correlation C_k of the data train with the filter is given by

$$C_k = \sum_{j=0}^{N-1} o_j q_{j+k} = \frac{1}{N} \sum_{l=0}^{N-1} \tilde{o}_l \tilde{q}_l^* \exp(2\pi i l k/N). \quad (59)$$

Here k is the lag, $\tilde{o}_l = \sum_{k=0}^{N-1} o_k \exp(-2\pi i l k/N)$ and $\tilde{q}_l = \sum_{k=0}^{N-1} q_k \exp(-2\pi i l k/N)$ are the discrete Fourier coefficients of the detector output and filter, and the second equality in (59) follows from the discrete correlation theorem. From this we see that the only computational cost involved in Weiner filtering is the inverse Fourier transform of the correlation since one stores the Fourier transforms of the templates, and the forward Fourier transform of the data is only computed once, the costs of multiplication being unimportant. The number of floating points operations involved in the fast Fourier transform is roughly $3N \log_2 N$.

Since in the discrete correlation formula (59) it is implicit that input functions are periodic while in reality they need not be, we get spurious correlation for lags not equal to zero. As a result the correlation apparently needs to be separately computed for every value of the lag. Fortunately this problem is circumvented by padding templates with zeroes, at the cost of a slight increase in the number of computations. so that correct correlation is obtained at least for a subset of values of the lag. Schutz [4] has shown that the optimum solution to the conflicting requirements of reduction in aliasing and reduction in the number of floating point operations involved in FFTs is to pad 75% of a template with zeroes. Padded templates give correct correlation for lags equal to the extent of padding. Consequently, if the data train is T s long with optimal padding we obtain correct correlation only for lags equal to $3T/4$. The number of floating point operations in the case of matched filtering $N_{\rm MF}$ is

$$N_{\rm MF} = n_f \times 3N \log_2 N \quad (60)$$

where n_f is the number of templates. Let us now compare the computational costs of Weiner filtering and periodogram for the example quoted in Sec. III D. In the case of matched filtering in order to obtain the correct correlation for a 12 s long duration it is necessary to process a data train that is 16 s long. For a sampling rate of 2 kHz we get $N = 2^{15}$ and for $t_C \in [0, 4]$ s we get $n_f = 1600$, giving $N_{\rm MF} = 2.5 \times 10^9$. We have seen in Sec. III B that in the case of periodogram the total number of floating point operations required to analyze a data train 12 seconds long is $\sim 5 \times 10^9$; the periodogram being computationally at worst a factor 2 more expensive than Weiner filtering. However, for this extra cost it introduces some flexibility in the analysis of gravitational wave data without sacrificing the detection probability. In the case of matched filtering, in order to save on computation time, all the templates have to be computed once and for all and stored. Thus, the memory requirement for their storage is pretty large though not beyond what the present-day computer-technology can offer. However, due to the large memory which the templates occupy there is a considerable amount of burden on the system bus in transfering data from and to CPU which can consequently slow down the computational speed. Moreover, if one decides to change the set of filters amidst a certain analysis all the requisite filters have to be re-generated. Periodogram has the advantage over Weiner filtering in these two aspects: It calls for no extra storage space apart from the (finely sampled) original data set. If a change in the set of test values of parameters and/or their numbers is required, say due to higher order post newtonian corrections, then it can be trivially achieved by redefining the resampling rates appropriately. The latter feature may prove useful for the case of Doppler de-modulation. If detailed simulations do show that periodogram is indeed as powerful as Weiner filtering in picking up weak signals then we should keep in mind some of its additional advantages. At worst periodogram analysis can be used as an independent statistic, as we will argue below, to increase confidence in a detection and to cross verify values of the parameters estimated.

Analogous to the random variables $C_0(X(\tau); \hat{\lambda})$ and $C_{\frac{\pi}{2}}(X(\tau); \hat{\lambda})$, in the case of matched filtering too we will have two random variables, say, $\eta_0(x(t); \hat{\lambda})$, $\eta_{\pi/2}(x(t); \hat{\lambda})$ corresponding to correlations of the data with templates of phase 0 and $\pi/2$, respectively. Since the resampling for folding will be nonuniform, the intersection of the set of samples picked up for folding and the corresponding set for matched filtering will have a small number of elements. It is expected, then, that in the absence of a signal,

$$\frac{\overline{C_i \eta_k}}{\sqrt{\overline{C_i^2}\;\overline{\eta_k^2}}} \ll 1; \quad i, k \in \{0, \pi/2\} \quad (61)$$

for white noise. This implies that the statistic obtained

from a periodogram is independent of that obtained from matched filtering. When the detector output consists only of noise then statistical independence means that a false alarm in the Weiner filtered output does not necessarily imply a false alarm in the periodogram based decision. Thus, the false alarm can be brought down if both the statistics are used in conjunction.

V. CONCLUSIONS

The use of matched filtering for the detection of gravitational wave forms emitted by in-spiraling binaries, though the optimum strategy, is computationally very expensive. The problem would be aggravated when higher order PN corrections are taken into account. Though it has been shown that one can get around this problem by a judicious choice of filter parameters, at least up to the $^{1.5}$PN level, the inclusion of higher order corrections may increase the number of templates quite a lot. A further increase in the number of templates required may come about when the seismic cutoff in the interferometric detectors is pushed down to a few Hertz. This will enable a larger integration time but will also make it necessary to correct for Doppler shifts due to the relative motion of the source and the Earth.

Therefore it is important to search for detection strategies which satisfy the twin requirements of being computationally less intensive than matched filtering but having a signal to noise ratio comparable with it. These two criteria may happen to be inconsistent with each other. We are not aware of such a result and hence feel the need to investigate every potential strategy individually. Our efforts in this direction led us to consider periodogram analysis as a serious candidate. Our analysis is restricted to the detection of *Newtonian* chirps embedded in *white* noise. We report the main results of this work below.

(a) *The enhancement in signal to noise ratio obtained in periodogram analysis is the same as in the case of matched filtering*

(c) *The detection statistic used in periodogram analysis is statistically independent from that used in matched filtering.* This implies that if both the statistics are used, then the confidence level of a detection can be increased. This result is strictly valid for the case of white noise and needs to be investigated further when the noise is colored.

(c) *As far as computational costs go, periodogram turns out to be as expensive as Weiner filtering.* The typical number of operations required $\sim 5 \times 10^9$ for 12sec of data whereas the corresponding number is $\sim 2.5 \times 10^9$ for matched filtering. The main reason is that for the periodogram, the resampling and folding of the data train has to be done for every value of the time-of-arrival used. While in matched filtering, the inverse transformation of the Fourier domain filter output takes care of the time-of-arrival in one go.

Another strategy which may fulfill the two objectives outlined above is the one suggested by Smith. Though we have not investigated the computational cost of this strategy in any detail, we expect that it will, at the least, be as expensive as periodogram analysis. This is because the problem of resampling the data train and subsequently processing it for every time-of-arrival is present here too. The number of operations for every resampled set is $\sim N\log_2 N$ where N is the number of points obtained on resampling. This is to be compared with $\sim N$ operations in the case of periodogram analysis.

It may be possible to reduce the computation involved in matched filtering by employing an efficient search algorithm, in parameter space, for the global maximum of the statistic instead of a serial search. In practice, there may exist several local maxima, the number and positions of which will depend on the specific realization of noise. Since the existence of local maxima degrades the performance of such search algorithms, their efficacy in this case needs to be investigated. Another approach with some promise is the use of a *warped* wavelet basis as far as the detection of chirps is concerned. Also, in this paper we do not address in any detail the problem of parameter estimation in the context of a periodogram. This is an important problem since the power of this technique would be fully tested only after we have the covariance matrix of errors. These issues will be taken up in a separate paper [20].

ACKNOWLEDGEMENTS

It is a pleasure to thank the members of the gravitational wave group at IUCAA, especially R. Balasubramanian, and Sanjeev Dhurandhar for many useful discussions. S.D.M. is supported by a CSIR fellowship.

[1] A. Abramovici, W.E. Althouse, R.W.P. Drever, Y. Gursel S. Kawamura, F.J. Raab, D. Shoemaker, L. Sievers, R.E. Spero, K.S. Thorne, R.E. Vogt, R. Weiss, S.E. Whitcomb and M.E. Zucker, *Science*, **256**, 325 (1992).

[2] C. Bradaschia, R. Delfabbro, A. Divirgilio, A. Giazotto, H. Kautzky, V. Montelatici, D. Passuello, A. Brillet, O. Cregut, and et.al. *Nucl. Inst. A.*, **289**, 518 (1990).

[3] K.S. Thorne, in *300 Years of Gravitation*, S.W. Hawking and W.Israel (eds.), (Cambridge Univ. Press, 1987).

[4] B.F. Schutz, in *The Detection of Gravitational Radiation*, edited by D. Blair (Cambridge, 1989) pp 406-427.

[5] A. Krolak, J.A. Lobo and B.J. Meers, Phys. Rev. D, **43**, 2470 (1991).

[6] L.S. Finn and D.F. Chernoff, Phys. Rev. D **47**, 2198 (1993).
[7] C. Cutler, T. A. Apostolatos, L. Bildsten, L. S. Finn, E. E. Flanagan, D. Kennefick, D. M. Markovic, A. Ori, E. Poisson, G. J. Sussman and K. S. Thorne, Phys. Rev. Lett. **70**, 2984 (1993).
[8] R. Balasubramanian and S. V. Dhurandhar, Phys. Rev. D **50**, 6080 (1994).
[9] K. D. Kokkotas, A. Królak, and G. Tsegas, Class. Quantum Grav. **11**, 1901 (1994).
[10] B. S. Sathyaprakash, Phys. Rev. D**50**, R7111 (1994).
[11] R. Flaminio, L. Massonnet, B. Mours, S. Tissot, D. Verkndt, M. Yvert, Astroparticle Physics, **2**, 235 (1994).
[12] S. Smith, Phys. Rev. D, **36**, 2901, (1987).
[13] A.G. Lyne, in *Gravitational Wave Data Analysis*, edited by B.F. Schutz (Kluwer, Dordrecht, 1989), pp. 95-103.
[14] L. Blanchet, T. Damour, B.R. Iyer, C. Will and A.G. Wiseman, Gravitational radiation damping of compact binary systems to second post-Newtonian order, submitted to Phys. Rev. Lett., (1995)
[15] Throughout this paper we use Geometrical units: $G = c = 1$.
[16] In what follows we denote the periodogram of a function of time by the same letter but in upper case. For instance, the periodogram of $x(t)$ is $X(\tau)$. In all periodograms and functions of τ constructed out of them it is to be understood that $0 \leq \tau < 1/f_0$.
[17] But now one has to match the periodogram of the detector output with a sinusoidal template.
[18] C.W. Helstrom, *Statistical Theory of Signal Detection*, 2nd. ed, (Pergamon Press, London, 1968).
[19] B.S. Sathyaprakash and S.V. Dhurandhar, Phys. Rev. D **44**, 3819 (1991).
[20] S.D. Mohanty and B.S. Sathyaprakash, in preparation.

FIG. 1. Development of relative phase of chirp wave forms mismatched in their chirp times is shown plotted for several wave forms with their chirp times in the range [1.98, 2.02] s. We have shown the number of cycles by which two wave forms differ as a function of time.

FIG. 2. The amplitude of the periodogram $\overline{A}(\tau)$ normalised to $\overline{A}(0)$ is shown plotted as a function of τf_0. The amplitude changes by a smaller amount for larger chirp times, which have a larger number of cycles.

FIG. 3. Contours of equal SNR $\rho(\hat{\lambda}, \lambda)$.

FIG. 4. Maximum, over t_a and Φ, of the SNR $C(\Delta\lambda)$ as a function of the signal chirp time t_C for several templates of chirp times t_C^k.

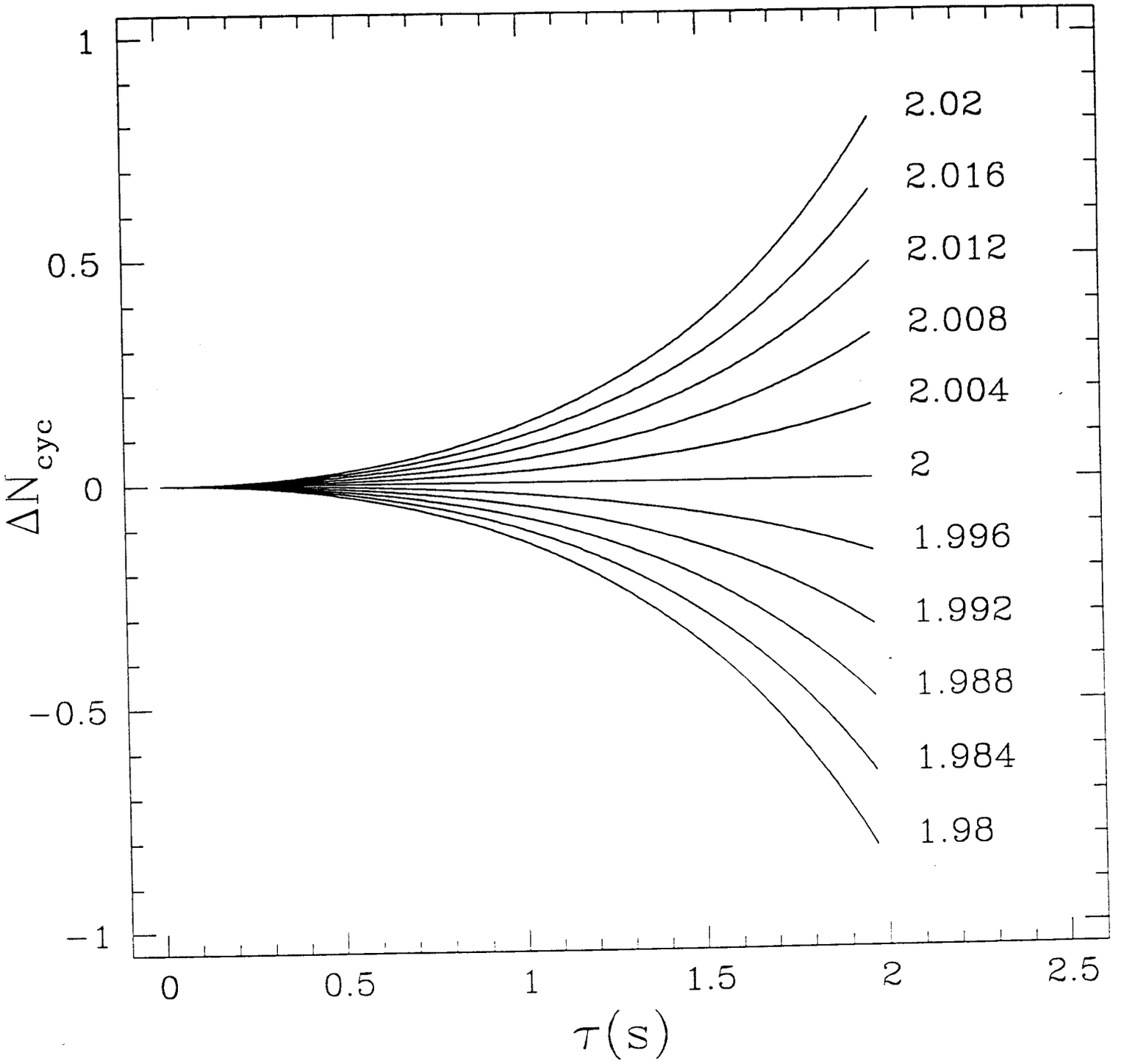
1
0.5
0
−0.5
−1
ΔN_{cyc}
0
0.5
1
1.5
2
2.5
τ(s)
2.02
2.016
2.012
2.008
2.004
2
1.996
1.992
1.988
1.984
1.98

Fig 1.

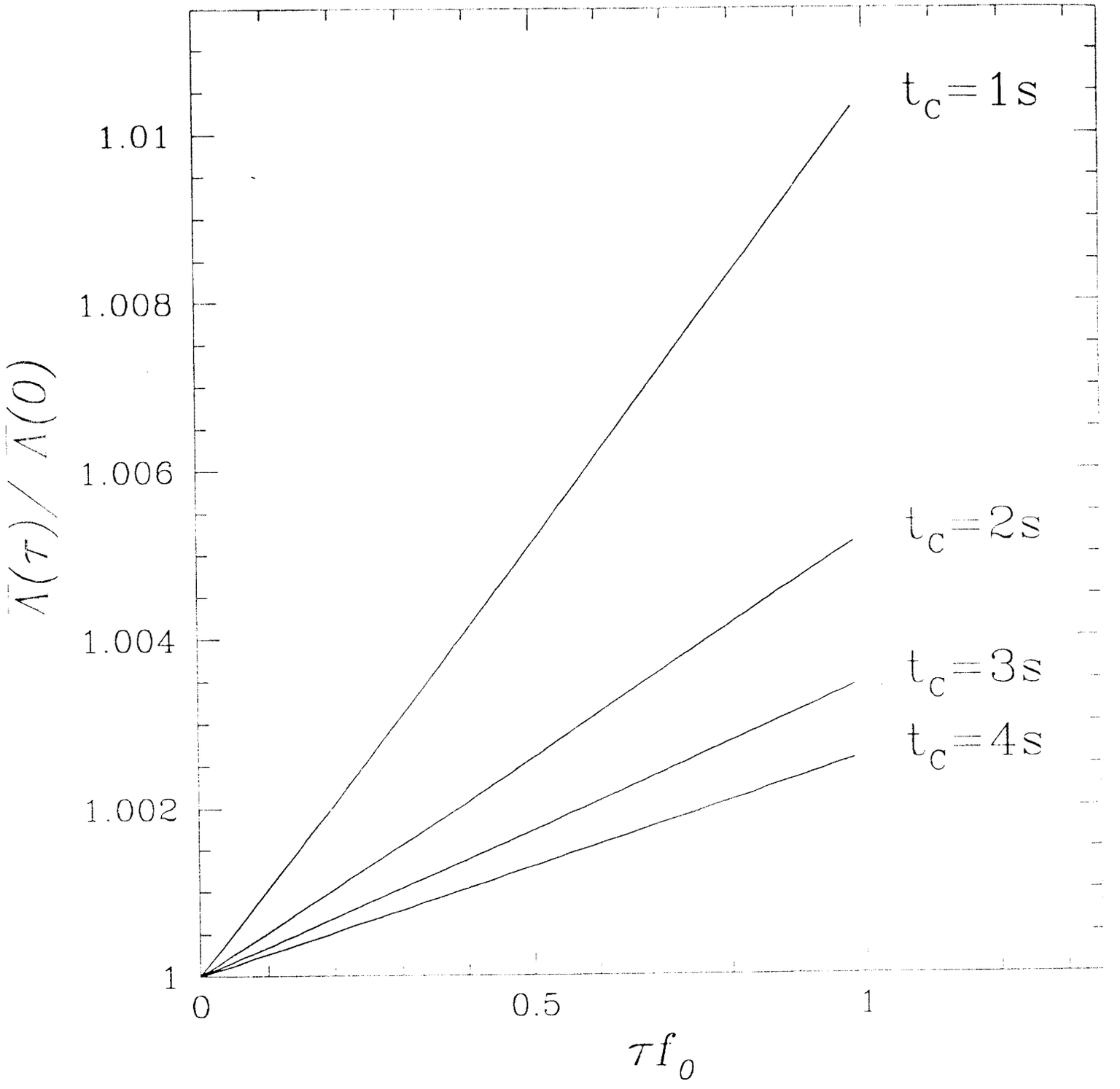
$t_c = 1s$
$t_c = 2s$
$t_c = 3s$
$t_c = 4s$
1.01
1.008
1.006
1.004
1.002
1
0
0.5
1
$\bar{\Lambda}(\tau) / \bar{\Lambda}(0)$
τf_0

Fig 2.

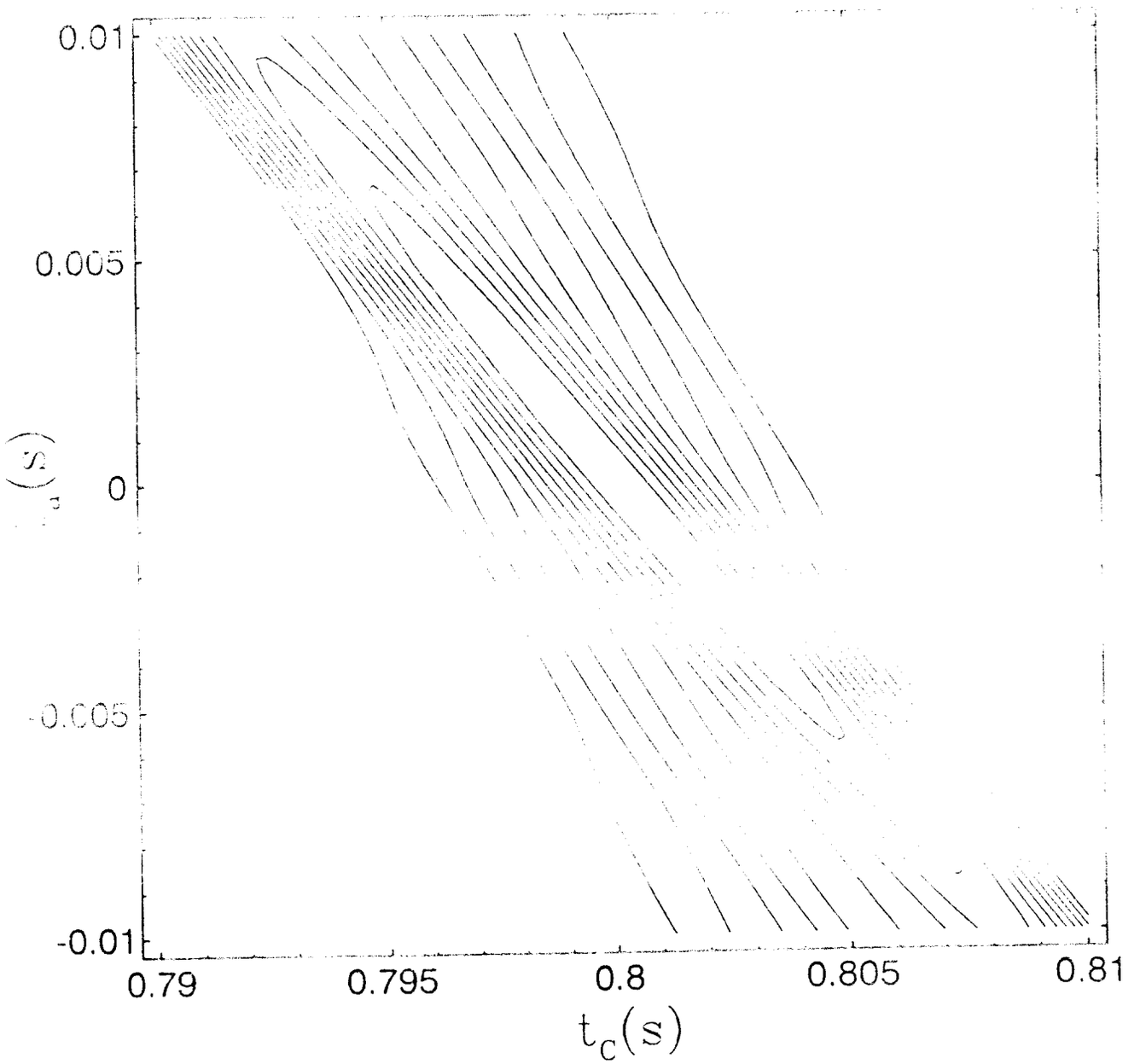

Fig 3.

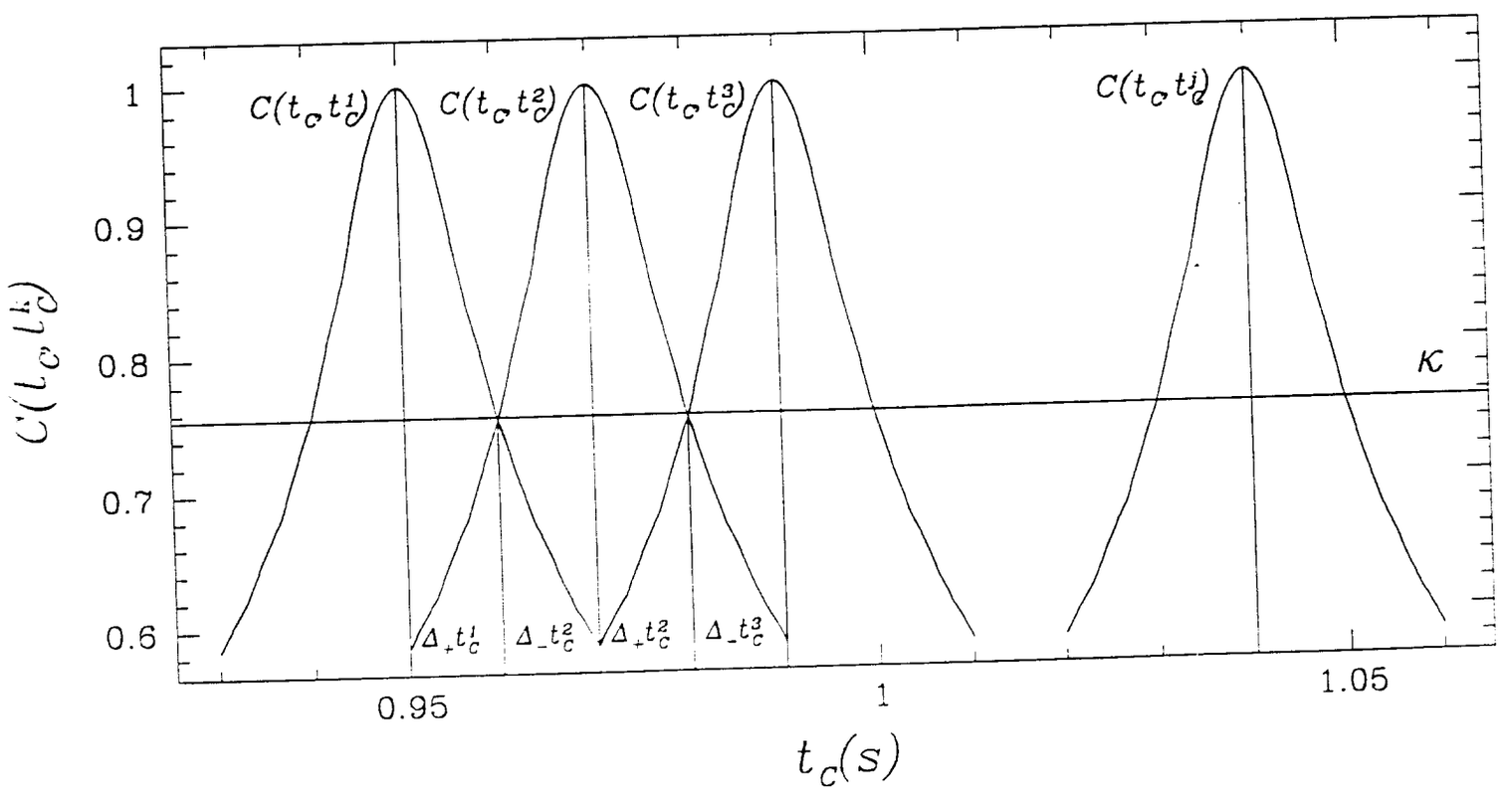
1
0.9
0.8
0.7
0.6
$C(L_C L_C^k)$
$C(t_C t_C^1)$
$C(t_C t_C^2)$
$C(t_C t_C^3)$
$C(t_C t_C^j)$
κ
$\Delta_+ t_C^1$
$\Delta_- t_C^2$
$\Delta_+ t_C^2$
$\Delta_- t_C^3$
0.95
1
1.05
$t_C(s)$

Fig 4.